Supporting Information
Rapid Synthesis of C-TiO_2: Tuning the Shape from Spherical to Rice Grain Morphology for Visible Light Photocatalytic Applications

Balaji Sambandam[a], Anupama Surenjan[b], Ligy Philip[b], and Thalappil Pradeep[a]

[a]DST Unit of Nanoscience and Thematic Unit of Excellence, Department of Chemistry, Indian Institute of Technology Madras, Chennai 600036, India and
[b]Department of Civil Engineering, Indian Institute of Technology Madras, Chennai 600036, India.

Table S1: Results from varying reaction time**

S.No	Time in min	Morphology	Crystalline phase
CT-13	10	spherical	Anatase
CT-14	18	spherical and oval	Anatase
CT-15	40	spherical and oval	Anatase

**Conditions: Volume: 80% ; Temperature: 150 °C; Concentrations: Same as in C1 (see Table 1), power: 400 W

Table S2: Results from varying the volume#

S.No	Volume	Morphology	Crystalline phase
CT-16	50%	spherical	Anatase
CT-17	40%	distorted spherical	Anatase
CT-18	30%	no specific morphology	Anatase

#Conditions: Temperature: 150 °C; Time: 30 min; Concentrations: Same as in C1; power: 400 W

Table S3: Results from varying the temperature$

S.No	Temp in (° C)	Morphology	Crystalline phase
CT-19	70	no specific morphology	Anatase
CT-20	100	no specific morphology	Anatase

$Conditions: Time: 30 min; Concentrations: Same as in C1; power: 400 W, Volume: 80%

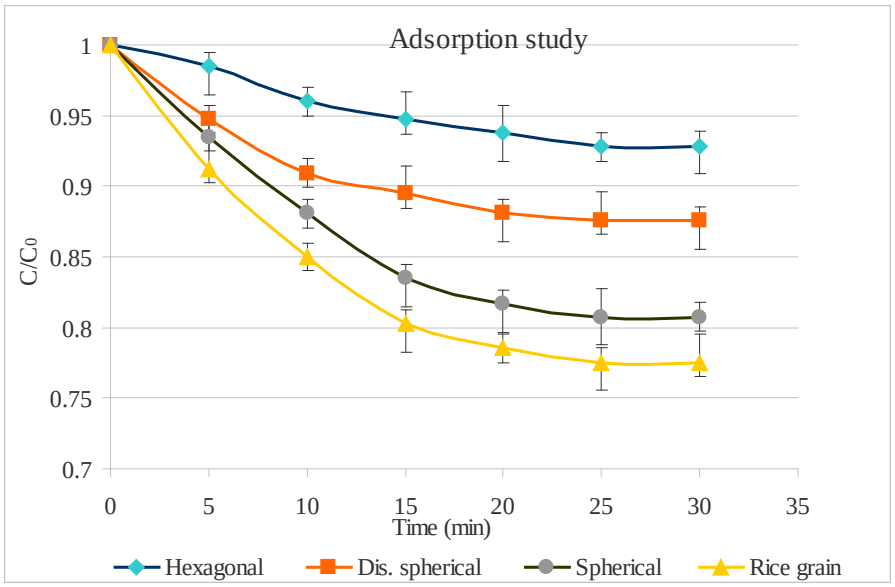

Figure S1. Removal of carbamazepine using different shapes of C-TiO_2 catalysts in dark.

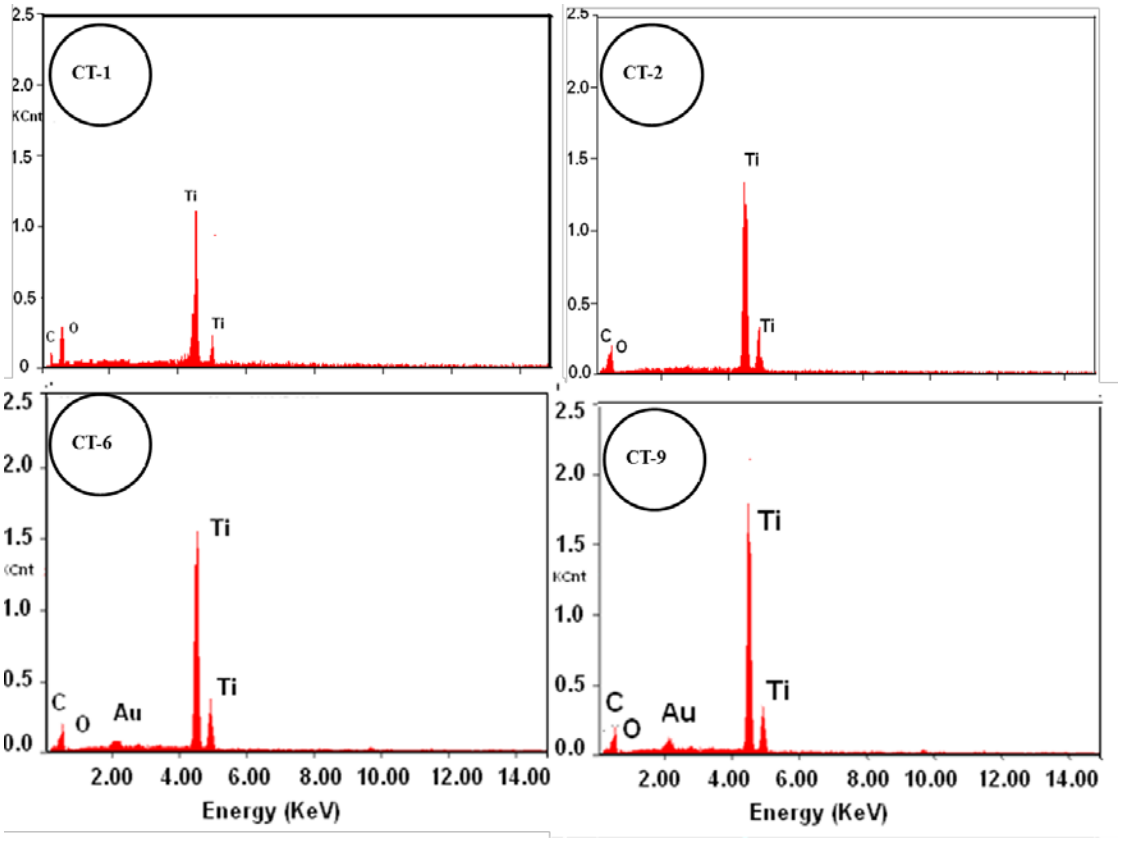

Figure S2. EDS pattern for four different morphologies of C-TiO_2.

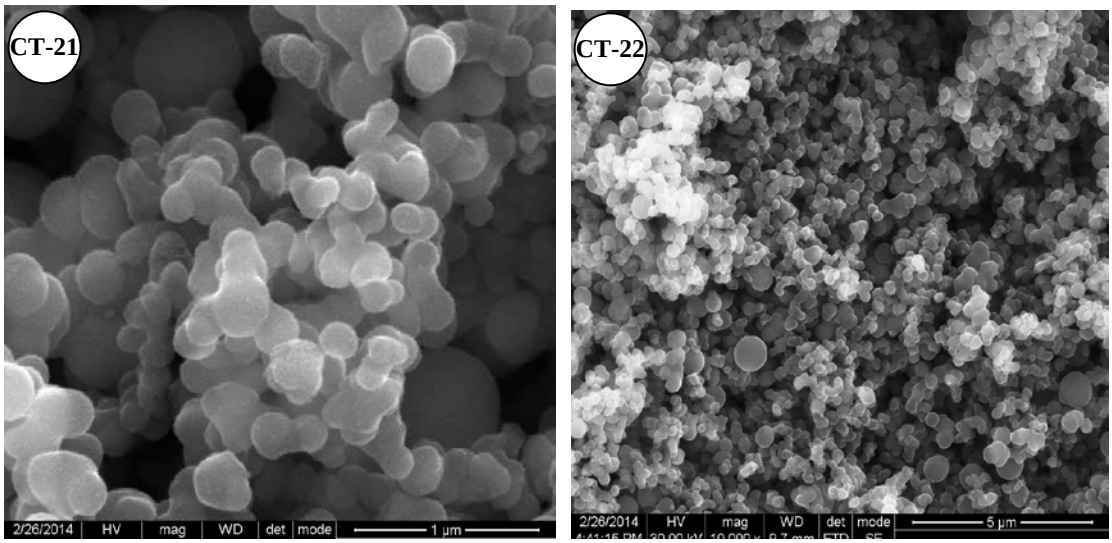

Figure S3. HRSEM images for C-TiO_2 at higher concentration of the ingredients.

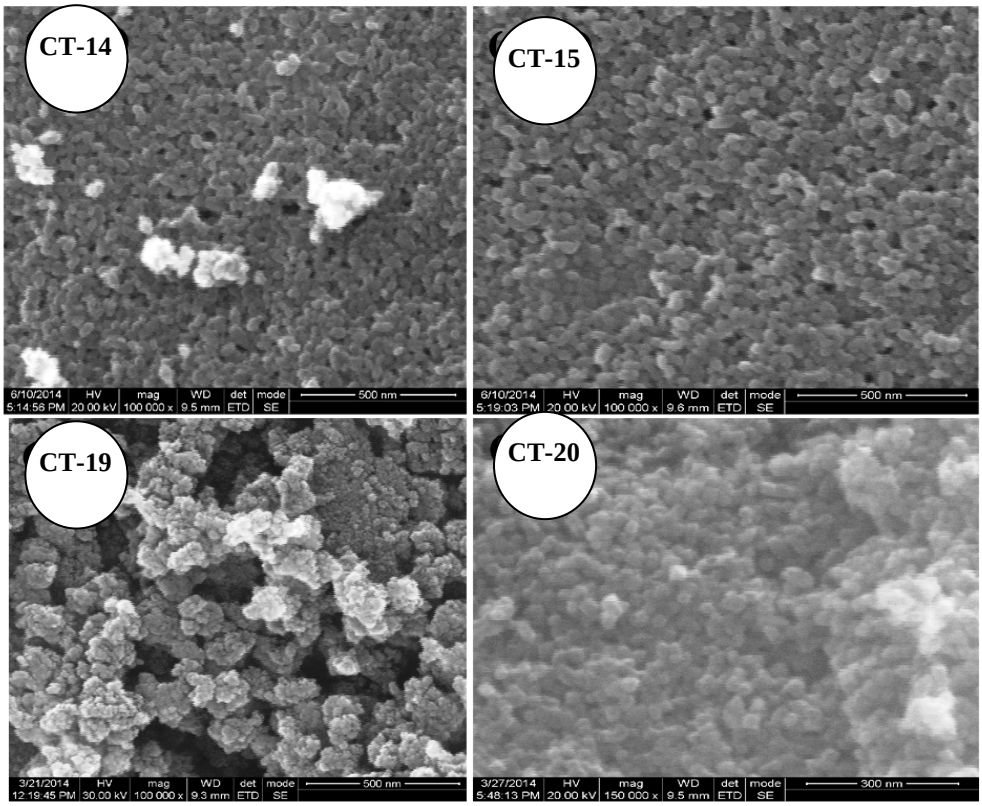

Figure S4. HRSEM images for C-TiO_2 of CT-14 and CT-15 (see Tables S1 and S3) showcasing time and temperature dependence of synthesis.

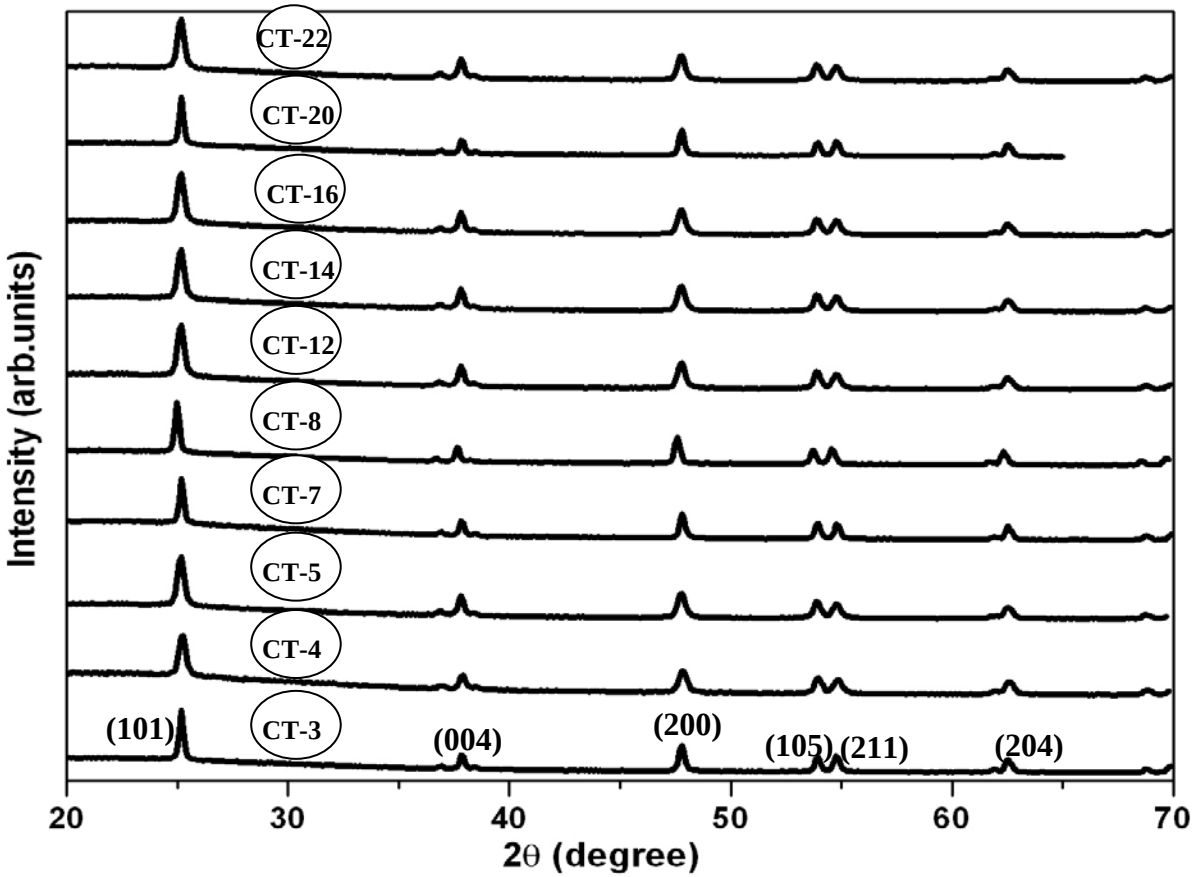

Figure S5. XRD profile for C-TiO_2 at various preparative conditions.

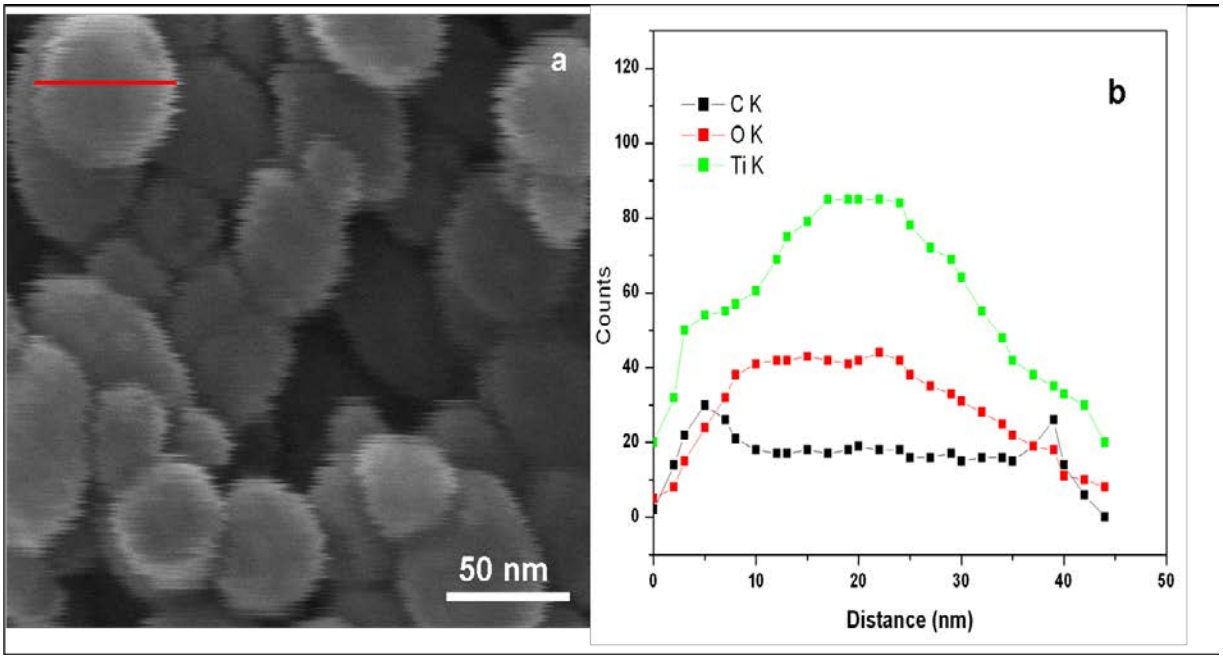

Figure S6. (a) HRSEM image of spherical shaped C-TiO_2 and (b) corresponding EDS line scan data for a single particle as marked by a red line in (a).

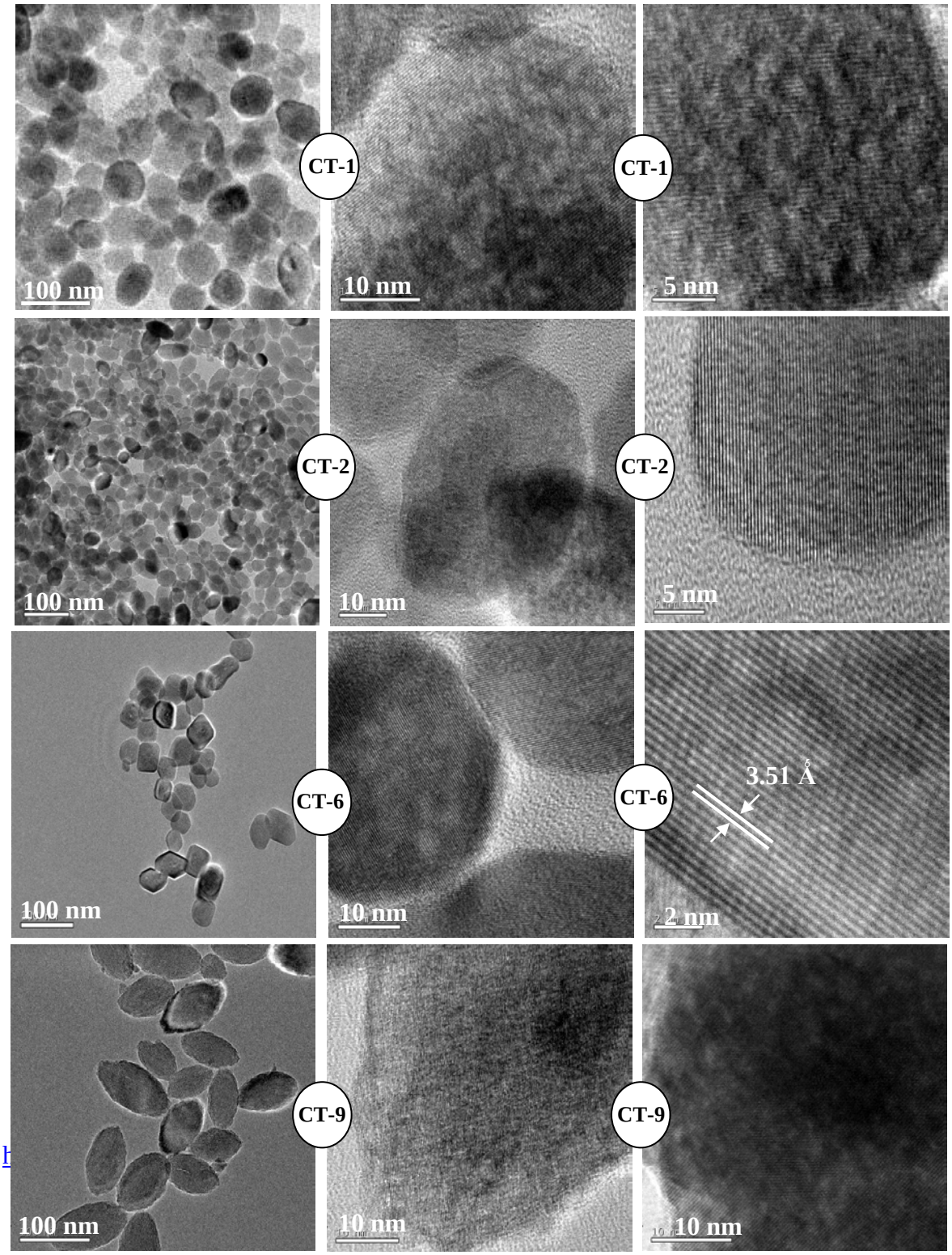

Figure S7. HRTEM images for the four different morphologies of C-TiO_2 nanocrystals.

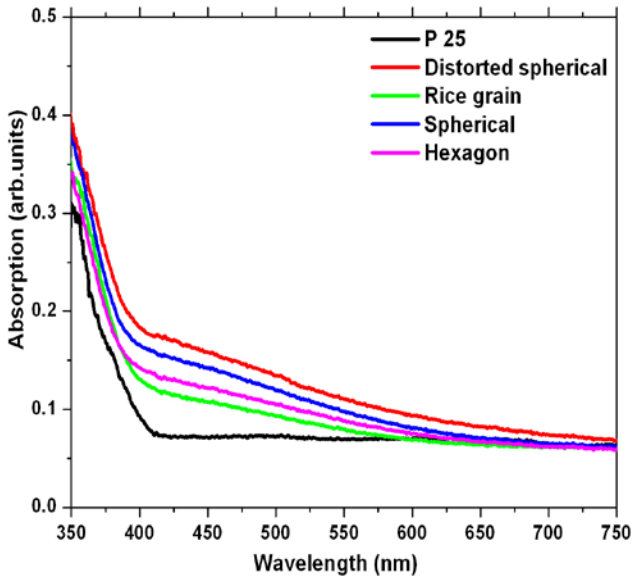

Figure S8. UV-vis diffuse reflectance profiles for four different morphologies of C-TiO_2 in comparison with P25 Degussa (bulk TiO_2).

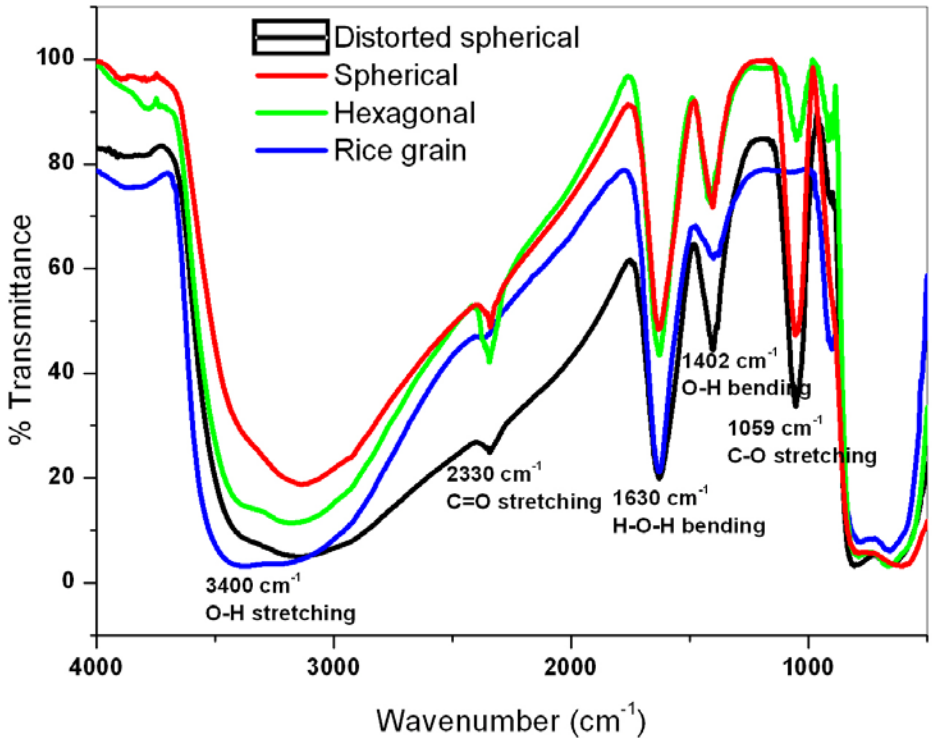

Figure S9. FT-IR spectra for C-TiO_2 of four different morphologies.

Table S4. BET surface area for the different morphologies of C-TiO_2

Sample code	Surface area, m^2/g	Pore volume, cc/g	Pore diameter, Å
Spherical (CT-1)	62	0.24	180
Distorted spherical (CT-2)	61	0.19	224
Hexagonal (CT-6)	33	0.18	190
Rice grain (CT-9)	229	0.17	36

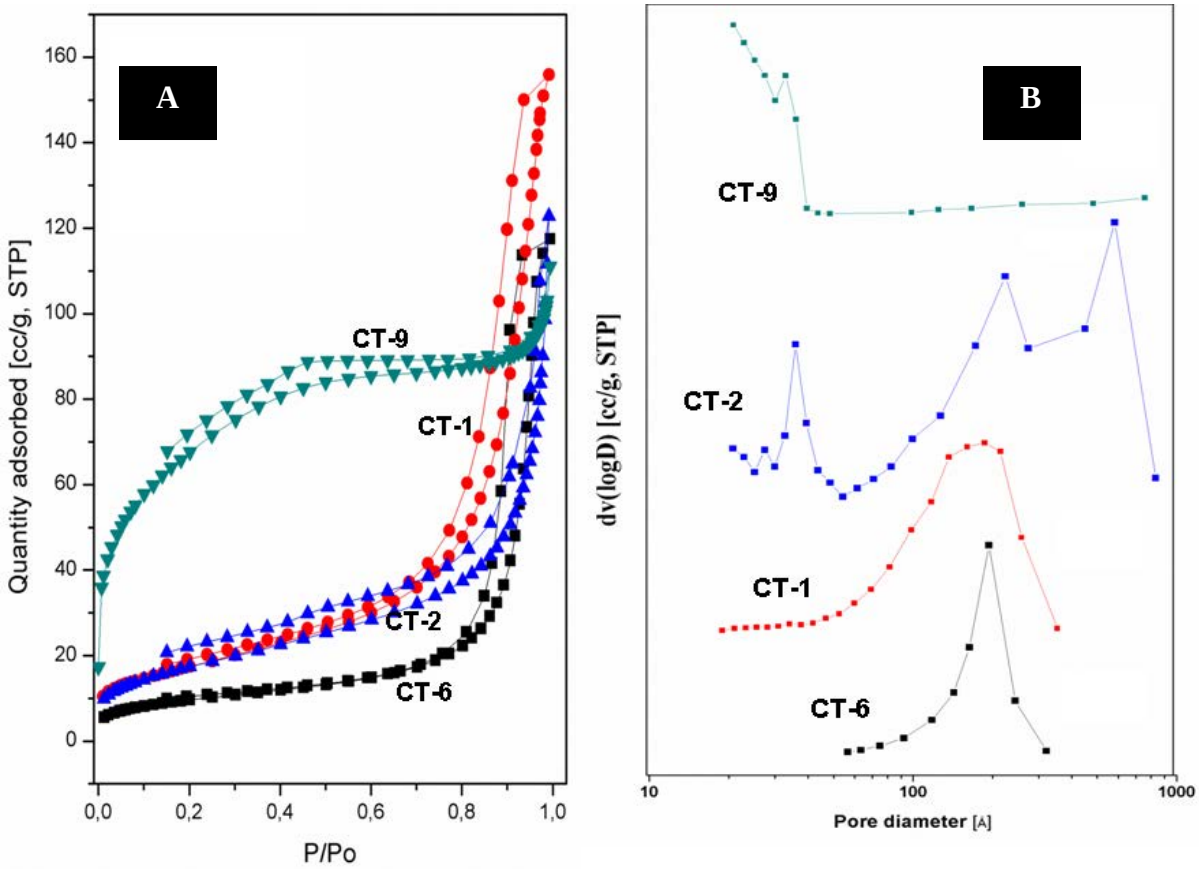

Figure S10. N_2-adsorption-desorption isotherm liner plot (A) and BJH desorption average pore diameter (B) for four different morphologies of C-TiO_2.

Table S5. Rate of degradation of Carbamazepine using different shaped C-TiO_2

Pollutant	Catalyst shape	R^2	K min^{-1}
	Rice grain (CT-9)	0.98	0.094
Carbamazepine	Spherical (CT-1)	0.99	0.059
(50µg/L)	Distorted spherical (CT-2)	0.99	0.044
	Hexagonal (CT-6)	0.97	0.020

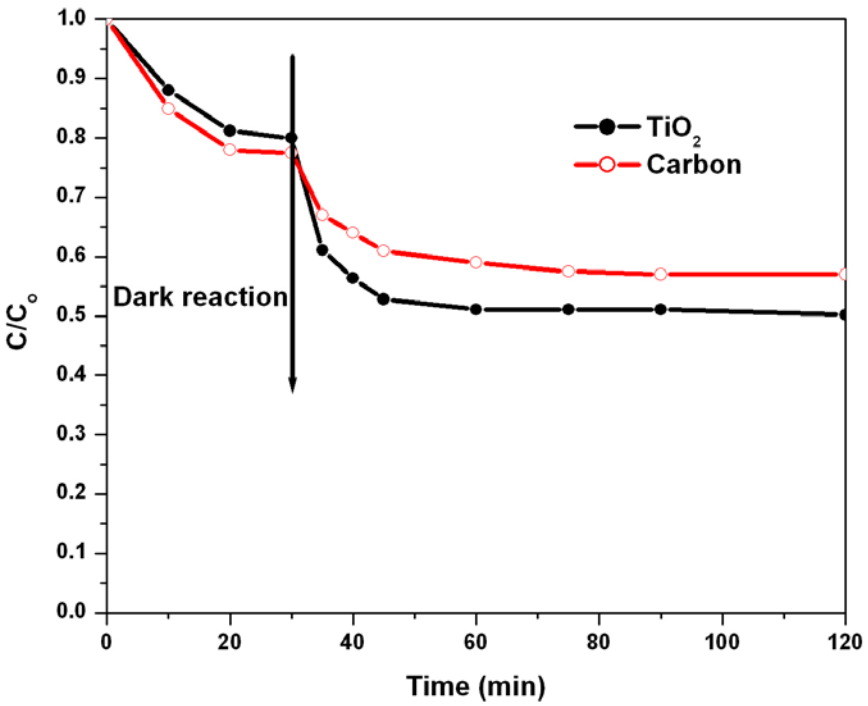

Figure S11. Photocatalytic activity for carbamazepine by TiO_2 and carbon prepared by CT-1 method.